10

Semi-active Vibration Control Based on Switched Piezoelectric Transducers

Hongli Ji, Jinhao Qiu and Pinqi Xia
Nanjing University of Aeronautics and Astronautics
China

1. Introduction

Vibration in modern structures like airplanes, satellites or cars can cause malfunctions, fatigue damages or radiate unwanted and loud noise (Simpson & Schweiger, 1998; Wu et al., 2000; Hopkins et al., 2000; Kim et al., 1999; Zhang et al., 2001; Hagood et al., 1990). Since conventional passive damping materials have reached their limits to damp vibration because it is not very effective at low frequencies and requires more space and weight, new control designs with novel actuator systems have been proposed. These so called smart materials can control and suppress vibration in an efficient and intelligent way without causing much additional weight or cost. The vast majority of research in smart damping materials has concentrated on the control of structures made from composite materials with embedded or bonded piezoelectric transducers because of their excellent mechanical-electrical coupling characteristics. A piezoelectric material responds to mechanical force by generating an electric charge or voltage. This phenomenon is called the direct piezoelectric effect. On the other hand, when an electric field is applied to the material mechanical stress or strain is induced; this phenomenon is called the converse piezoelectric effect. The direct effect is used for sensing and the converse effect for actuation. The methods of vibration control using piezoelectric transducers can be mainly divided into three categories: passive, active, and semi-active. Passive control systems, which use the *R-L* shunting (Hagood & Crawley, 1991; Hollkamp, 1994), are simplest among the three categories, but their control performance is sensitive to the variations of the system parameters. Moreover, the passive control systems usually need large inductance in low frequency domain, which is difficult to realize. Active control systems require high-performance digital signal processors and bulky power amplifiers to drive actuators, which are not suitable for many practical applications.

In order to overcome these disadvantages, several semi-active approaches have been proposed. Wang et al. (1996) studied a semi-active *R-L* shunting approach, in which an adaptive inductor tuning, a negative resistance and a coupling enhancement set-up lead to a system with damping ability. Davis et al. (1997, 1998) developed a tunable electrically shunted piezoceramic vibration absorber, in which a passive capacitive shunt circuit is used to electrically change the piezoceramic effective stiffness and then to tune the device response frequency. Clark, W. W. (1999) proposed a state-switched method, in which piezoelements are periodically held in the open-circuit state, then switched and held in the short-circuit state, synchronously with the structure motion.

Source: Vibration Control, Book edited by: Dr. Mickaël Lallart,
ISBN 978-953-307-117-6, pp. 380, September 2010, Sciyo, Croatia, downloaded from SCIYO.COM

Another type of semi-active control, which has been receiving much attention in recent years, is called pulse switching technique (Richard et al., 1999, 2000; Onoda et al., 2003; Makihara et al., 2005). It consists in a fast inversion of voltage on the piezoelement using a few basics electronics, which is synchronized with the mechanical vibration. In the methods proposed by Richard et al. (1999) the voltage on the piezoelectric element is switched at the strain extrema or displacement extrama of vibration. These methods are called Synchronized Switch Damping (SSD) techniques. On the other hand, in the method proposed by Onoda and Makihara the switch is controlled by an active control theory and it is called active control theory based switching technique here (Onoda et al., 2003; Makihara et al., 2005).
In this chapter, the semi-active control methods based on state-switched piezoelectric transducers and pulse-switched piezoelectric transducers are introduced (Qiu et al., 2009). The semi-active approaches have several advantages compared to the passive and active methods: it is not sensitive to the variation of the parameters of system, and its implementation is quite simple, requiring only few small electronic components. It may use inductors, but much smaller than the ones needed by passive technique. So the control system is more compact compared with active control and passive control.

2. Modeling of a structural system with piezoelectric transducers

2.1 Equivalent SDOF model

A mechanical model based on a spring-mass system having only one degree of freedom gives a good description of vibrating behavior of a structure near a resonance (Badel et al., 2006; Ji et al., 2009a). The following differential equation is established assuming that the global structure including piezoelectric elements is linearly elastic:

$$M\ddot{u} + C\dot{u} + K_E u = \sum F_i \tag{1}$$

where M represents the equivalent rigid mass, C is the inherent structural damping coefficient, K_E is the equivalent stiffness of the structural system, including the host structure and piezoelectric elements in short-circuit, u is the rigid mass displacement and $\sum F_i$ represents the sum of other forces applied to the equivalent rigid mass, comprising forces applied by piezoelectric elements. The equivalent stiffness K_E can be expressed as

$$K_E = K_s + K^{sc} \tag{2}$$

where K_s is the stiffness of the host structure and the K^{sc} is the stiffness of the piezoelectric transducer in short circuit. Piezoelectric elements bonded on the considered structure ensure the electromechanical coupling, which is described by

$$F_p = -\alpha V \tag{3}$$

$$I = \alpha\dot{u} - C_0\dot{V} \tag{4}$$

where F_p is the electrically dependent part of the force applied by piezoelectric elements on the structure, C_0 is the blocked capacitance of piezoelectric elements, α is the force factor, and I is the outgoing current from piezoelectric elements. M, C_0, α and K_E can be deduced from piezoelectric elements and structure characteristics and geometry.
Finally, $\sum F_i$ applied to the rigid equivalent mass comprises F_p and an external excitation force F. Thus, the differential equation governing the mass motion can be written as

$$M\ddot{u} + C\dot{u} + K_E u = F - \alpha V \tag{5}$$

The following energy equation is obtained by multiplying both sides of the above equation by the velocity and integrating it over the time variable.

$$\int_0^T F\dot{u}dt = \frac{1}{2}M\dot{u}^2\Big|_0^T + \frac{1}{2}K_E u^2\Big|_0^T + \int_0^T C\dot{u}^2 dt + \int_0^T \alpha V\dot{u}dt \tag{6}$$

This equation exhibits that the provided energy is divided into kinetic energy, potential elastic energy, mechanical losses, and transferred energy. In the steady-state vibration, the terms of potential energy and kinetic energy in Eq. (6) disappear. The provided energy is balanced by the energy dissipated on the mechanical damper and the transferred energy, which corresponds to the part of mechanical energy which is converted into electrical energy. Maximizing this energy amounts to minimize the mechanical energy in the structure (kinetic + elastic).

If the frequency of excitation equals the resonance frequency of the system, the velocity of the mass, $\dot{u}$, can be considered to be in phase with the excitation force $F(t)$. In that case, the provided energy and the energy dissipated on mechanical damper are

$$\int_0^T F\dot{u}dt = F_M u_M \pi \quad \text{and} \quad \int_0^T C\dot{u}^2 dt = C\omega_0 u_M^2 \pi \tag{7}$$

where F_M is the amplitude of the excitation force.

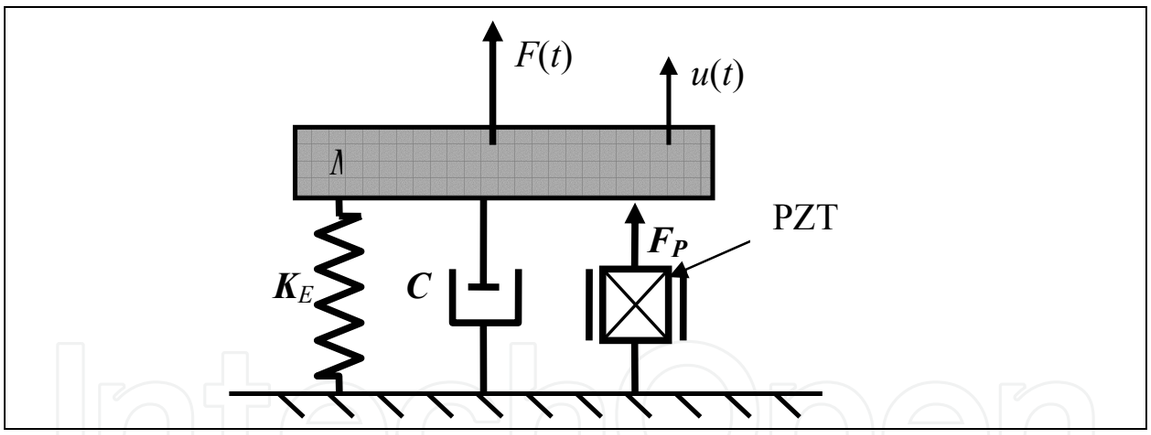

Fig. 1. A single SDOF with a piezoelectric transducer

2.2 A system with a shunt circuit

In passive control, the piezoelectric transducer in a structural system is connected to an electrical impedance (Hagood, 1991). In semi-active control, the piezoelectric transducer is usually connected to a switching shunt circuit, which is electrically nonlinear (Clark, 2000). When the piezoelectric transducer is connected to an electrical impedance Z^{SU}, Eq. (4) becomes

$$\tilde{V} = \frac{s\alpha^2 Z^{SU}}{sC_0 Z^{SU} + 1}\tilde{u} \tag{8}$$

in the Laplace domain, where $\tilde{V}$ and $\tilde{u}$ are the Laplace transformation of V and u, and s is the Laplace variable. Substitution of Eq. (8) into the Laplace transformation of Eq. (5) gives the transfer function from excitation force F to displacement response u as follows

$$\tilde{u}/\tilde{F} = \frac{1}{Ms^2 + Cs + K_E + \dfrac{s\alpha^2 Z^{SU}}{sC_0 Z^{SU} + 1}} \tag{9}$$

where $\tilde{F}$ is the Laplace transformation of F. In passive control, optimal control performance is achieved by tuning the electrical impedance, Z^{SU}, of the shunt circuit. However, the control performance of a passive control system deteriorates drastically when the Z^{SU} is detuned. Hence a passive control system is very sensitive to the variation of the system parameters and has low robustness.

Several semi-active approaches have been proposed to overcome the disadvantages of passive control systems. One is to adaptively tune the impedance, Z^{SU}, of the shunt circuit. The second is to switch the shunt circuit between the states with different impedances. The third is to invert the voltage on the piezoelectric transducer by synchronically pulse-switching the shunt circuit.

2.3 Different states of piezoelectric transducer

(1) Short circuit condition

In the short circuit condition, the impedance of the shunt circuit connected to the piezoelectric transducer is zero (Z^{SU}=0) and no electric power is dissipated, either. In the frequency domain, Equations (8) and (9) can be expressed as

$$\tilde{V} = 0\,,\ \frac{\tilde{u}}{\tilde{F}} = \frac{1}{\left(K_E - M\omega^2 + jC\omega\right)} \tag{10}$$

It is assumed that at the resonance frequency the force F and the speed $\dot{u}$ are in phase (this is a good approximation for structures with low viscous losses). The resonance angular frequency and the amplitude of the displacement are given by

$$\omega_0^{sc} = \sqrt{\frac{K_E}{M}}\,,\ u_M = \frac{F_M}{C\omega_0}\,. \tag{11}$$

where F_M is this amplitude of the driving force. In the short circuit condition, the provided energy is balanced by the mechanical loss.

(2) Open circuit condition

In the open circuit condition of the piezoelectric elements, the impedance of the shunt circuit is infinity (Z^{SU}=∞) and no electric power is dissipated, either. In the frequency domain, Equations (8) and (9) can be expressed as

$$\tilde{V} = \frac{\alpha}{C_0}\tilde{u}\,,\ \frac{\tilde{u}}{\tilde{F}} = \frac{1}{\left(K_E + \dfrac{\alpha^2}{C_0} - M\omega^2 + jC\omega\right)} \tag{12}$$

For the same reason as for the short circuit case, the resonance angular frequency and the amplitude of the displacement are given by.

$$\omega_0^{oc} = \sqrt{\frac{K_E + \frac{\alpha^2}{C_0}}{M}}\ ,\ u_M = \frac{F_M}{C\omega_0^{oc}}\ . \tag{13}$$

Obviously, the stiffness of the piezoelectric transducer in the open circuit condition is

$$K^{oc} = K^{sc} + \frac{\alpha^2}{C_0}\ . \tag{14}$$

The piezoelectric transducer exhibits higher stiffness in the open circuit condition and the resonance frequency of the system in open circuit condition is higher than that in the short circuit condition. The voltage on the piezoelectric transducer and the displacement and velocity of the mass are illustrated in Fig.2. In this state, the net converted energy from mechanical to electrical in a cycle of vibration is zero, that is, the last term in Eq. (6) is zero.

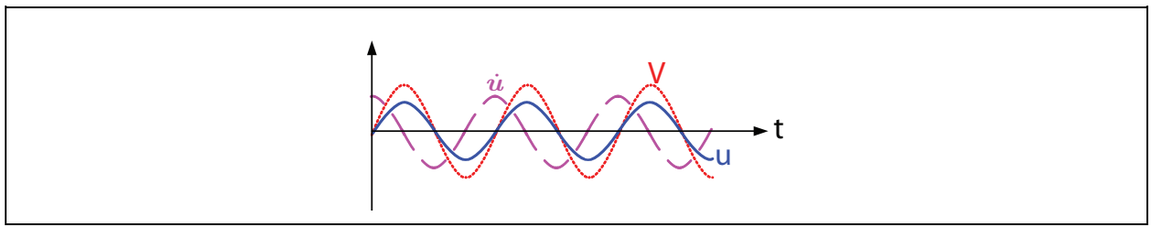

Fig. 2. Voltage, displacement and velocity in the open circuit condition

Obviously, the difference between the resonance frequency in the short circuit condition and that in the open circuit condition is due to the electro-mechanical coupling of the piezoelectric transducer in the structure. To quantitatively characterize its electro-mechanical property, the following parameter, k_{struct}, is defined as the electro-mechanical coupling factor of the structure:

$$k_{struct} = \frac{\left(\omega_0^{oc}\right)^2 - \left(\omega_0^{sc}\right)^2}{\left(\omega_0^{sc}\right)^2}\ . \tag{15}$$

The resonance frequencies, ω_0^{oc} and ω_0^{sc}, of the structure with the piezoelectric transducer under open and short circuit conditions, respectively, can easily be measured experimentally. Hence the electro-mechanical coupling factor of the structure can easily be estimated from experimentally results. After k_{struct} is obtained, the force factor, α, can easily be calculated from the following equation:

$$\alpha = k_{struct}\omega_0^{sc}\sqrt{C_0}\ . \tag{16}$$

(3) Resistive shunt condition

When the piezoelectric transducer is shunted by a resistor R, that is, $Z^{SU}=R$, Equations (8) and (9) can be expressed as

$$\tilde{V} = \frac{j\rho\omega/\omega_n}{j\rho\omega/\omega_n + 1} \cdot \frac{\alpha^2}{C_0}\tilde{u} \,,$$

$$\frac{\tilde{u}}{\tilde{F}} = \frac{1}{\left(K_E - M\omega^2 + jC\omega + \dfrac{j\rho\omega/\omega_n}{j\rho\omega/\omega_n + 1} \cdot \dfrac{\alpha^2}{C_0}\right)} \tag{17}$$

in the frequency domain, where ω_n is an arbitrary angular frequency for non-dimensionalization and $\rho = \omega_n C_0 R$ is the non-dimensional resistance. The condition R=0 corresponds to short circuit and R=∞ corresponds to the open circuit condition.
Resistive shunt has been widely used in passive damping based on piezoelectric transducers. An optimal resistance can be obtained by minimizing the magnitude of the transfer function from $\tilde{F}$ to $\tilde{u}$ at the resonance frequency of the system. In the next section the control performance of the state-switched approach is compared with that of the resistive shunt.

3. The state-switched approach

The state-switched method has been successfully used in semi-passive vibration absorbers (Cunefare, 2002) and semi-passive vibration damping using piezoelectric actuator (Clark 1999, 2000; Corr & Clark 2001). Only the state-switched approach using piezoelectric actuators is discussed in this section. In the state-switched approach using piezoelectric actuators, a piezoelectric actuator is switched between the high- and low-stiffness states using a simple switching logic to achieve vibration suppression, essentially storing energy in the high-stiffness state and dissipating a part of the that energy in the switching process between the low-stiffness state and high-stiffness state. As shown in the Section 2.3, the piezoelectric transducer has different stiffness for different electrical boundary conditions (short circuit or open circuit). Different from the pulse-switched approach introduced in the next section, this approach keeps the piezoelectric element in each of the high- and low-stiffness states for one quarter-cycle increments.
The energy loss in a state-switched system can be explained by a mass-spring system as shown in Fig. 3 (Corr & Clark, 2001). The stiffness of the spring, K^*, in the system can be switched between two states: K^{HI} and K^{LO}, with $K^{\mathrm{HI}} > K^{\mathrm{LO}}$. As the mass move away from its equilibrium position, the stiffness of the spring is set to K^{HI}. When the mass reaches its maximum displacement the potential energy is at a maximum:

$$U_{\max} = K^{\mathrm{HI}} u_M^2 \tag{18}$$

At this point, the stiffness of the variable spring is changed from K^{HI} to K^{LO}. Now the potential energy of the system is less than before. The difference in energy is

$$\Delta U = \frac{1}{2}\left(K^{\mathrm{HI}} - K^{\mathrm{LO}}\right) u_M^2 \,. \tag{19}$$

Hence, there is ΔU less potential energy to be converted back to kinetic energy, that is, the system has lost some of its total energy. The variable spring is left in the K^{LO} state until the mass goes back to its original equilibrium point. At this time, the variable spring is again changed to K^{HI} state and the cycle repeats itself.

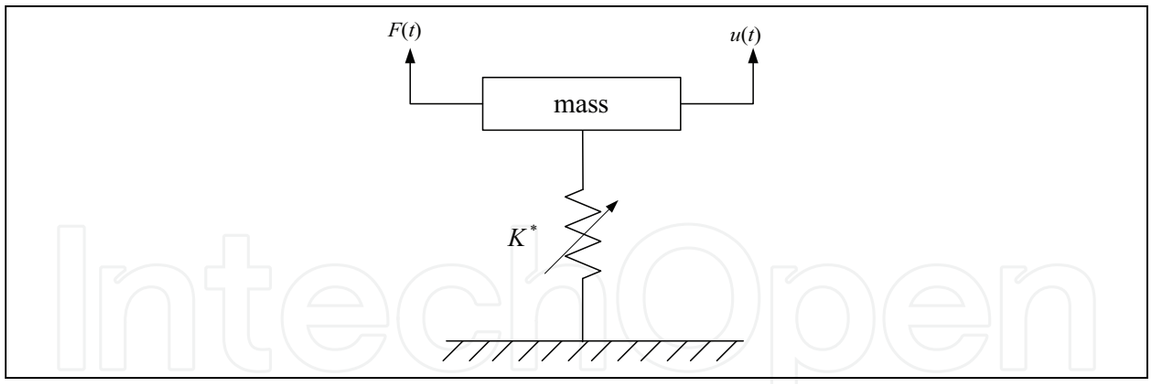

Fig. 3. A SDOF system with a variable spring

In theory, one could continuously vary the resistance in the circuit in real time to obtain a completely variable semi-active system. An alternative is to simply switch between states of the system. The two most straightforward scenarios are shown in Fig. 4(b) and 4(c), where switching occurs between the open and short circuit states (OC-SC), and between the open and resistive shunt states (OC-RS). (Note that switching between the short circuit and resistive shunt states will not be explored because neither of these states exhibits high-stiffness.) State-switching of the actuator is based on the following logic: Given the single degree-of-freedom system shown in Fig. 4, when the system is moving away from equilibrium, or

$$u\dot{u} > 0 \tag{20}$$

the circuit is switched to the high-stiffness state (open circuit), and when the system is moving toward equilibrium,

$$u\dot{u} < 0 \tag{21}$$

then the system is switched to the low-stiffness and/or dissipative state (short or resistive circuit). So during a full cycle of motion, switching occurs four times, once after each quarter cycle. At equilibrium the system is switched to a high stiffness, then at peak motion it is switched back to low stiffness and it returns to equilibrium to complete the half-cycle. At equilibrium again the system is switched to high stiffness, and the switching process repeats over the next half-cycle. This has the effect of suppressing deflection away from equilibrium, and then at the end of the deflection quarter-cycle, dissipating some of the stored energy so that it is not given back to the system in the form of kinetic energy.

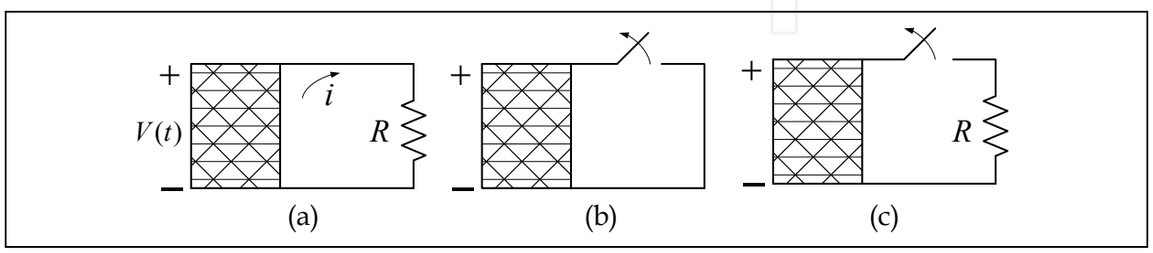

Fig. 4. Schematic of three piezoelectric configurations used in this study: (a) Passive resistive shunt; (b) State-switched: Open-circuit to short circuit; (c) State-switched: Open-circuit to resistive circuit

Now the SDOF system in Fig. 1 is considered. The mass is under excitation of a harmonic force $F(t)$ with an angular frequency of ω and its response is assumed to be a harmonic vibration of the same frequency. The piezoelectric transducer is switched between open circuit and short circuit using the switching strategy in Eqs. (20) and (21). The energy dissipated in a full cycle of vibration due to the switching actions is

$$\begin{aligned} E_{cycle}^{dis} &= \int_0^{T/4} K^{oc} u\dot{u}dt + \int_{T/4}^{T/2} K^{sc} u\dot{u}dt + \int_{T/2}^{3T/4} K^{oc} u\dot{u}dt + \int_{3T/4}^{T} K^{sc} u\dot{u}dt \\ &= (K^{oc} - K^{sc})u_M^2 \\ &= \frac{\alpha^2}{C_0} u_M^2 \end{aligned} \tag{22}$$

In the open-circuit case, deflection stores energy by way of the mechanical stiffness and by the capacitance of the device, which also appears as a mechanical stiffness. When the system is then switched to the short circuit state, the charge stored across the capacitor is shunted to ground, effectively dissipating that portion of the energy, and the effective stiffness is decreased. Since the provided energy is balanced by the mechanical loss and the energy dissipated by the switched shunted circuit, the following equation holds when the system is excited at the resonance frequency:

$$F_M u_M \pi = C\omega_0 u_M^2 \pi + \frac{\alpha^2}{C_0} u_M^2 . \tag{23}$$

The displacement amplitude of vibration is

$$u_M = \frac{F_M}{C\omega_0 + \dfrac{\alpha^2}{\pi C_0}} . \tag{24}$$

To quantitatively evaluate the damping effect of a control method, a performance index A is defined as follows

$$A = 20\log\left(\frac{\text{vibration amplitude with control}}{\text{vibration amplitude without control}}\right) . \tag{25}$$

The performance index of the state-switched control for a single-frequency vibration is given by

$$A_{\text{State-swithing}} = 20\log\left(\frac{C\omega_0}{C\omega_0 + \dfrac{\alpha^2}{\pi C_0}}\right) . \tag{26}$$

If on the other hand, the circuit is switched to the resistive shunt, then the electrical charge is dissipated through the resistor, and the effective stiffness is also decreased (an added benefit is that additional damping is obtained while the resistor is in the circuit during the next quarter cycle, so in some cases the OC-RS system can perform better than the OC-SC system.)

The damped impulse response of the OC-SC system can be compared to that of the other two systems of interest, that is, the RS system and the OC-RS system [Clark 2000]. The resistor used in both the RS circuit and that in the OC-RS circuit are chosen to be optimal. The results are shown in Fig. 5. Note that for the impulse response, it is better to use a resistor in the circuit during state-switching. It is also shown that slightly better damping can be achieved with the passive resistive shunt circuit. The effective damping ratios were calculated for each case by logarithmic decrement and are shown in Table 1.

System	Effective Damping Ratio
Passive Resistive Shunt	0.22
State-Switched OC-SC	0.12
State-Switched OC-RS	0.19

Table 1. Effective damping ratios for passive and state-switched systems

Even though the passive resistive shunt system provides slightly better performance than the state-switched systems for the optimized cases, it is interesting to note that the results change significantly when the resistors are no longer optimized. Simulations were performed on the impulse response of the same three systems when the mass and actuator material compliance are dramatically changed but the resistance values are held at their previous optimal values. The results showed that the state-switched systems are less sensitive to the change, seeing very little change in performance, with the OC-RS case still providing slightly better performance (note that the OC-SC case can be thought of as a lower limit on damping performance), but the passive resistive shunt case is much worse than before.

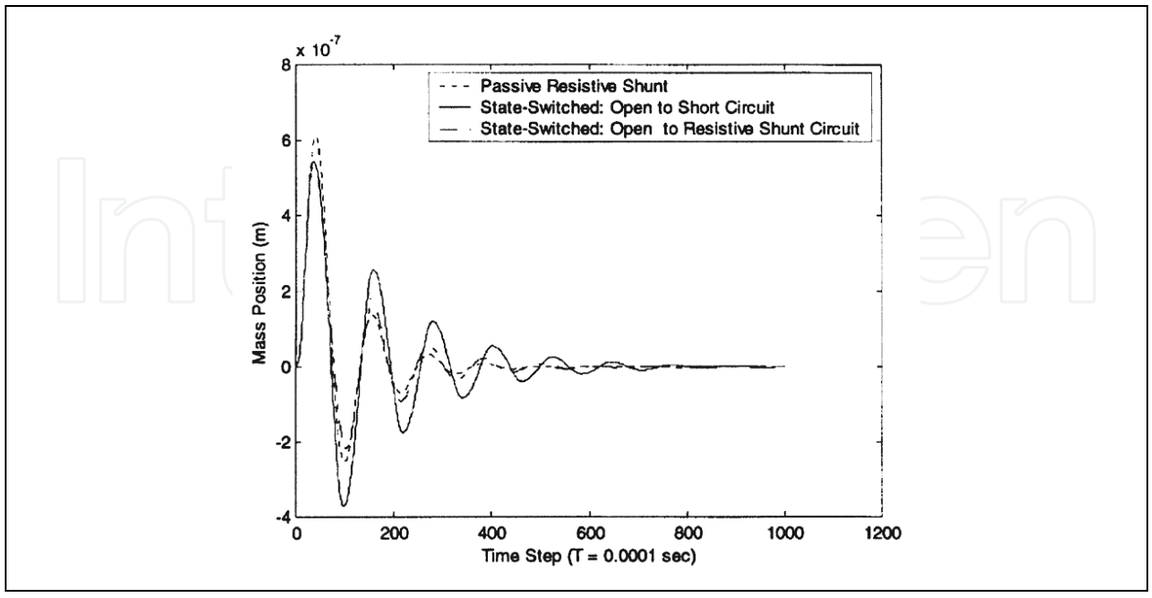

Fig. 5. Impulse response of passive resistive shunt, the OC-RS state switched, and OC-RS state-switched systems using optimal resistance

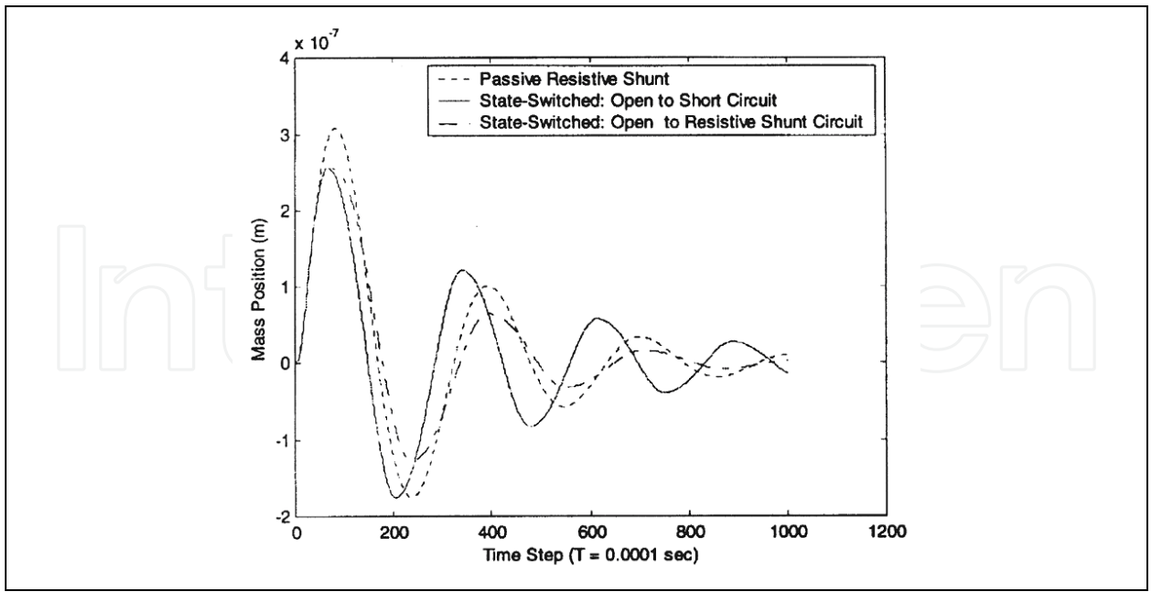

Fig. 6. Impulse response of passive resistive shunt, the OC-RS state switched, and OC-RS state-switched systems with non-optimal resistance

4. The pulse-switch methods

4.1 The Synchronized Switch Damping technique

The synchronized switch damping (SSD) method, also called pulse-switched method, consists in a nonlinear processing of the voltage on a piezoelectric actuator. It is implemented with a simple electronic switch synchronously driven with the structural motion. This switch, which is used to cancel or inverse the voltage on the piezoelectric element, allows to briefly connect a simple electrical network (short circuit, inductor, voltage sources depending on the SSD version) to the piezoelectric element. Due to this process, a voltage magnification is obtained and a phase shift appears between the strain in piezoelectric patch and the resulting voltage. The force generated by the resulting voltage is always opposite to the velocity of the structure, thus creating energy dissipation. The dissipated energy corresponds to the part of the mechanical energy which is converted into electric energy. Maximizing this energy is equivalent to minimizing the mechanical energy in the structure.

(1) The synchronized switch damping on short circuit

Several SSD techniques have been reported. The simplest is called SSDS, as shown in Figure 7(a), which stands for Synchronized Switch Damping on Short circuit (Richard et al., 1999, 2000). The SSDS technique consists of a simple switching device in parallel with the piezoelectric patch without other electric devices. The switch is kept open for most of the time in a period of vibration. It is closed when the voltage reaches a maximum (corresponding to a maximum of the strain in the piezoelectric patch) to dissipate all the electric energy in a short time (much shorter than the period of vibration) and then opened again. The voltage on the piezoelectric transducer is shown in Fig. 7(b). The maximum voltage on the piezoelectric transducer is

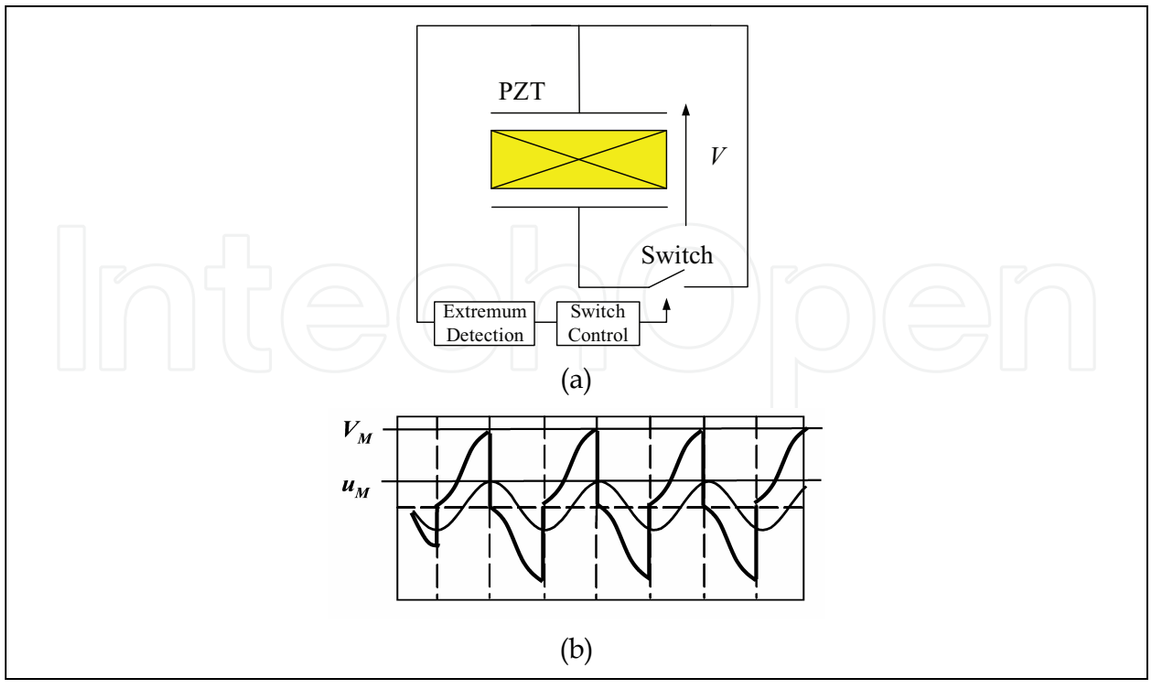

Fig. 7. The principle of SSDS technique

$$V_{Max} = \frac{2\alpha}{C_0} u_M \tag{27}$$

which is twice as large as that in the open circuit condition.
The maximum electric energy stored in the piezoelectric transducer can easily be calculated from the voltage in Eq. (27). This energy is dissipated when the voltage is discharged to zero at the maximum displacement point. In each cycle of mechanical vibration, the piezoelectric transducer is discharged twice. Hence, in the SSDS technique, the transferred energy E_t in a period of single-frequency vibration is given by

$$E_t = \frac{4\alpha^2}{C_0} u_M^2 \tag{28}$$

The performance index of the SSDS damping for a single-frequency vibration is given by

$$A_{SSDS} = 20\log\left(\frac{C\omega_0}{C\omega_0 + \frac{4\alpha^2}{C_0\pi}}\right) \tag{29}$$

The above expressions exhibit that more energy is dissipated by the SSDS than by the state-switched shunt circuit in a single cycle of mechanical vibration and SSDS yields better control performance.

(2) The synchronized switch damping on inductor

To further increase the dissipated energy, the SSDI technique (synchronized switch damping on inductor) as shown in Fig. 8a has been developed by Richard et al. (2000),

Guyomar et al. (2001) and Petit et al. (2004). In the SSDI approach, an inductor is connected in series with the switch. Because the piezoelectric patch and the inductor constitute a *L*-*C* resonance circuit, fast inversion of the voltage on the piezoelectric patch is achieved by appropriately controlling the closing time and duration of the switch. The switch is closed at the displacement extremes, and the duration of the closed state is half the period of the *L*-*C* circuit. This leads to an artificial increase of the dissipated energy. The period of the *L*-*C* circuit is chosen to be much smaller than that of the mechanical vibration. The following relation holds between the voltage before inversion, V_M, and that after inversion, V_m,

$$V_m = \gamma V_M \,, \tag{30}$$

where $\gamma \in [0,1]$ is the voltage inversion coefficient. The inversion coefficient γ is a function of the quality factor of the shunt circuit. The larger the quality factor is, the larger the voltage inversion coefficient is. A typical value of γ is between 0.6 to 0.9.

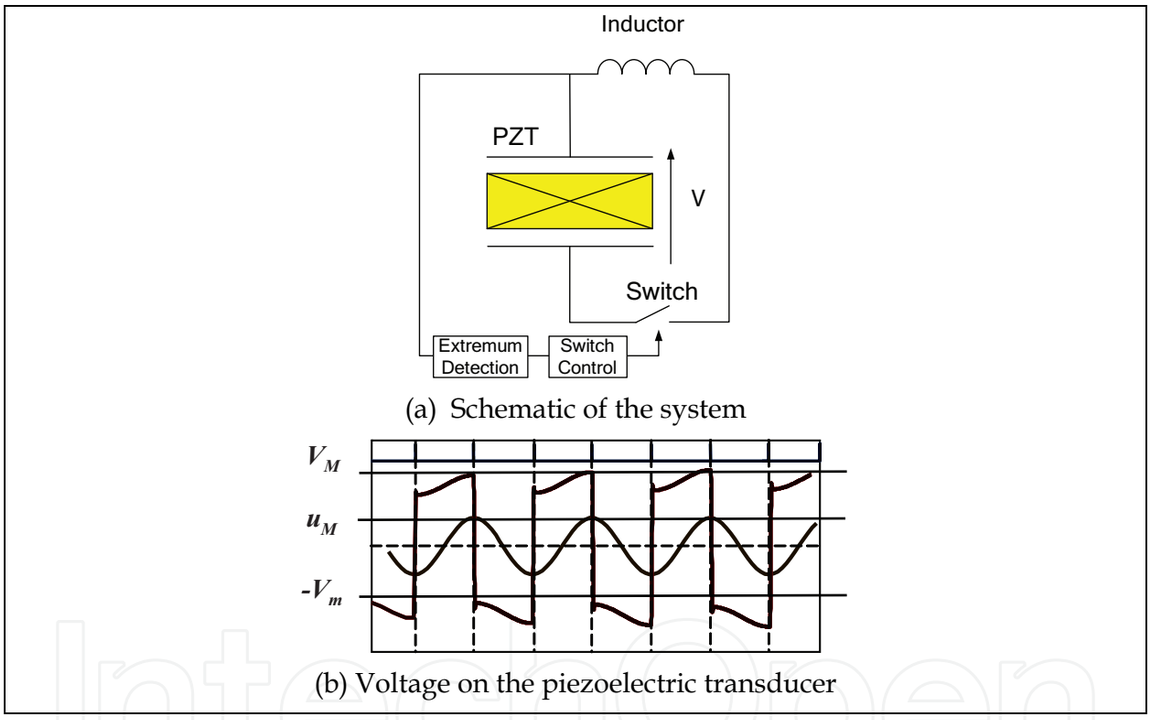

Fig. 8. The principle of SSDI technique

As shown in Fig. 8(b), in the steady-state vibration the voltage on piezoelectric transducer increases from V_m to V_M between two switching points due to mechanical strain. Hence their difference is V_{Max} given by Eq. (27). From these relationships, the absolute value of the average voltage between two switching points is

$$\frac{1}{2}(V_m + V_M) = \frac{1+\gamma}{1-\gamma}\frac{\alpha}{C_0}u_M \tag{31}$$

It indicates that the average voltage on the piezoelectric transducer has been amplified by a factor of $(1+\gamma)/(1-\gamma)$. The dissipated energy E_t during a period of single-frequency vibration is given by

$$E_t = \frac{4\alpha^2}{C_0}\frac{1+\gamma}{1-\gamma}u_M^2 \tag{32}$$

Compared with Eq. (28) the transferred energy has also been magnified by a factor of $(1+\gamma)/(1-\gamma)$ (Badel et al., 2005). If the voltage inversion coefficient is 0.9, its value is 9.5. Hence, much better control performance can be achieved with SSDI. The theoretical damping value of the SSDI technique for a single-frequency vibration is

$$A_{SSDI} = 20\log\left(\frac{C\omega_0}{C\omega_0 + \frac{4\alpha^2}{\pi C_0}\frac{1+\gamma}{1-\gamma}}\right). \tag{33}$$

4.2 The active control theory based switching law

Onoda and Makihara proposed a new switching law based on active control method (Onoda et al., 2003; Makihara et al. 2007c). As an example, the LQR (linear quadratic regulator) control law was used in their studies. The state equation of the plant to be controlled is assumed to be

$$\dot{\mathbf{z}} = \mathbf{A}\mathbf{z} + \mathbf{D}\mathbf{f} + \mathbf{B}\mathbf{Q} \tag{34}$$

where z is the state variable, $\boldsymbol{A}$, $\boldsymbol{B}$ and $\boldsymbol{C}$ are state matrices, $\boldsymbol{f}$ is the external disturbance, and $\boldsymbol{Q}$ is the control input, which is the charges on the piezoelectric elements. A linear quadratic regulator is designed to minimized the performance index

$$J = \int \left(\mathbf{z}^T\mathbf{W}_1\mathbf{z} + \mathbf{Q}^T\mathbf{W}_2\mathbf{Q}\right)dt \tag{35}$$

where $\boldsymbol{W}_1$ and $\boldsymbol{W}_2$ are weight matrices. The control input can be expressed in the following form:

$$\mathbf{Q}_T = \mathbf{F}\mathbf{z}\ . \tag{36}$$

The regulator $\boldsymbol{F}$ is given by

$$\mathbf{F} = \mathbf{W}_2^{-1}\mathbf{B}^T\mathbf{P} \tag{37}$$

where $\boldsymbol{P}$ is a positive definite solution of

$$\mathbf{P}\mathbf{B}\mathbf{W}_2^{-1}\mathbf{B}^T\mathbf{P} - \mathbf{A}^T\mathbf{P} - \mathbf{P}\mathbf{A} - \mathbf{W}_1 = 0\ . \tag{38}$$

Usually the value of z is difficult to measure and they estimated by an observer. When the estimated value of z is used, the active control input is obtained from

$$\mathbf{Q}_T = \mathbf{F}\hat{\mathbf{z}}\ . \tag{39}$$

where $\hat{\mathbf{z}}$ is the estimated value of z. Once the value of $\boldsymbol{Q}_T$ is obtained, the switch in the shunt circuit for the ith piezoelectric actuator is controlled based on Q_{Ti}, which is the ith component in the $\boldsymbol{Q}_T$, according to the switch control law discussed below.

It should be noted that in a semi-active control system, damping effect is achieved by switching shunt circuit, not by applying the control input $\boldsymbol{Q}_T$ as in active control. In order to

obtain damping effect, a possible strategy to control the switch is to turn the switch on and off so that the charge Q_i on the ith piezoelectric element traces Q_{Ti} as closely as possible. However, in many cases, a large gain results in quick vibration damping. Therefore, the switch is controlled such a way that $\boldsymbol{Q}$ becomes as large, that is, positive, as possible when $\boldsymbol{Q_T}$ is positive, and as small, that is, negative, as possible when $\boldsymbol{Q_T}$ is negative. The study by Onoda et al. (1997) has shown that this strategy is more effective than tracing $\boldsymbol{Q_T}$, although the difference between their performances is small.

Based on the above discussion, the following control law can be obtained for switched R shunt of a piezoelectric element: Turn on the switch when

$$Q_T V < 0\,, \tag{40}$$

and turn off the switch when

$$Q_T V > 0\,, \tag{41}$$

where V is the voltage on the piezoelectric patch.

The switch control law for a piezoelectric element with a switched L-R shunt can be expressed in the following form: Turn on the switch when

$$Q_T V < 0\,, \tag{42}$$

and turn it off when

$$Q_T \dot{Q} < 0\,. \tag{43}$$

Note that any active control theory can be used to obtain Q_T of a piezoelectric though LQR control method has been used as an example above.

5. The SSDV approach

5.1 The classical SSDV technique

In order to further increase the damping effect, a method called SSDV (SSDV stands for synchronized switch damping on voltage) as shown in Fig. 9 was proposed by Lefeuvre et al. (2006), Makihara et al. (2005), Faiz et al. (2006), and Badel et al., (2006). In the case of the SSDV, a voltage source V_{cc} is connected to the shunting branch, in series with the inductor, which can magnify the inverted voltage and hence improve the control performance. The absolute value of average voltage on piezoelectric transducer between two switching actions is (Badel, , et al., 2006)

$$V = (\frac{\alpha}{C_0} u_M + V_{cc}) \frac{1+\gamma}{1-\gamma}\,. \tag{44}$$

The dissipated energy during one period of vibration is a function of u_M and V_{cc} as follows:

$$E_t = (\frac{4\alpha^2}{C_0} u_M^2 + 4\alpha u_M V_{cc}) \frac{1+\gamma}{1-\gamma}\,. \tag{45}$$

The theoretical value of the SSDV damping is then given by

$$A_{SSDV} = 20\log\left(\frac{C\omega_0}{C\omega_0 + \frac{4\alpha^2}{C_0\pi}\frac{1+\gamma}{1-\gamma}} \times \left(1 - \frac{4}{\pi}\frac{1+\gamma}{1-\gamma}\frac{\alpha V_{cc}}{F_M}\right)\right), \tag{46}$$

where F_M is the amplitude of excitation force F_e. The SSDV technique can achieve better vibration control performance than SSDI, but a stability problem arises due to the fact that the voltage source is kept constant. Equation (46) shows that under a given excitation force, the value of voltage source V_{cc} that theoretically totally cancels the vibration can be found. This particular value is

$$V_{cc\max} = \frac{\pi}{4\alpha}\frac{1-\gamma}{1+\gamma}F_M . \tag{47}$$

This is also the maximum voltage that can be applied in this excitation condition. Applying a voltage higher than $V_{cc\max}$ leads to instability (experimental results actually show that stability problems occur before reaching this critical value).

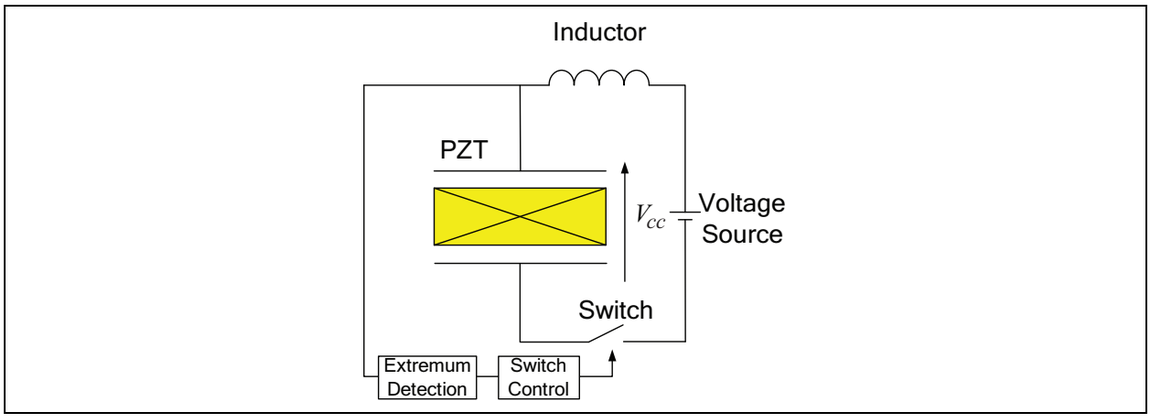

Fig. 9. The principle of SSDV technique

5.2 Adaptive SSDV techniques

Equation (47) shows that $V_{cc\max}$ is proportional to the amplitude of the excitation. Hence if the voltage is adjusted according to the amplitude of the excitation, the stability problem can be solved. Accordingly the enhanced and adaptive SSDV techniques, in which the voltage is adjusted according to the amplitude of excitation, have been developed. In a real system, the amplitude of the excitation is usually unknown, but we can measure the vibration amplitude of the structure.

(1) Enhanced SSDV

In the enhanced SSDV proposed by Badel et al. (2006) the voltage source is proportional to the vibration amplitude as shown in following equation.

$$V_{cc} = -\beta\frac{\alpha}{C_0}u_M , \tag{48}$$

where β is the mentioned voltage coefficient. In the Enhanced SSDV, the dissipated energy E_t during a period can be expressed as

$$E_t = \frac{4\alpha^2}{C_0}(1+\beta)\frac{1+\gamma}{1-\gamma}u_M^2 . \tag{49}$$

Compared with the classical SSDV technique, the enhanced SSDV increases the transferred energy, which results in an increase in the vibration damping. The theoretical value of damping of the enhanced SSDV is given by

$$A_{SSDV_{enh}} = 20\log\left(\frac{C\omega_0}{C\omega_0 + \frac{4\alpha^2}{C_0\pi}(1+\beta)\frac{1+\gamma}{1-\gamma}}\right) . \tag{50}$$

Equation (50) shows that, for a given value of parameter β, the damping is not sensitive to the amplitude of the applied force. This is the critical point of the enhanced SSDV. But it must be noted that for large value of β, the above theoretical expressions are no longer valid because the displacement of high-order modes cannot be neglected any longer compared to the fundamental one. From the experimental results it has been found that the optimal value of the voltage coefficient β depends on many factors such as the noise level of the measured signal, the property of the switch, et al. Hence, in order to achieve optimal control performance, the voltage coefficient should be adjusted adaptively according to the vibration amplitude and other experimental conditions.

(2) Derivative-based adaptive SSDV

An adaptive enhanced SSDV technique, in which the voltage coefficient is adjusted adaptively to achieve optimal control performance, has been proposed by Ji et al. (2009a). The basic principle of the adaptive SSDV technique is that the coefficient β is adjusted based on the sensitivity of the vibration amplitude with respect to β: the more the vibration amplitude is sensitive to β, the more β is increased. If the variation of amplitude is Δu_{Mi} due to an increment of the voltage coefficient $\Delta\beta_i$, the sensitivity is defined as $\Delta u_{Mi}/\Delta\beta_i$. The increment of the voltage coefficient, $\Delta\beta_{i+1}$, in the next step is defined as

$$\Delta\beta_{i+1} = -\eta\frac{\Delta u_{Mi}}{\Delta\beta_i} , \tag{51}$$

where η is the convergence rate factor. The larger the factor η is, the faster the convergence rate is. But when η is too large, the iteration process may become unstable. The physical meaning of the algorithm defined in Eq.(51) is similar to the Newton-Raphson method in numerical analysis.

Since $\Delta u_{Mi}/\Delta\beta_i$ is an approximation of the derivative of amplitude u_M with respect to β, this approach is called derivative-based adaptive SSDV. In the real system, $\Delta\beta_i$ is not updated in each cycle of vibration because of the noise in the measured amplitude. Instead, $\Delta\beta_i$ is kept constant for n cycles and the amplitudes u_{Mk} (k=1,…,n) are recorded. A parabolic curve is then fitted from the points u_{Mk} and the slope at the final point u_{Mn} is defined as the sensitivity.

(3) LMS-based adaptive SSDV

In the derivative-based adaptive SSDV, the voltage coefficient β is optimized to achieve good damping control performance. Actually, the final goal of optimizing voltage coefficient

β is to obtain the optimal voltage. A novel adaptive SSDV method based on LMS algorithm to adjust the voltage source directly or voltage coefficient was proposed by Ji et al. (2009b).
In the LMS-based adaptive SSDV, a FIR filter is used to optimize the voltage V_{cc} or the voltage coefficient β. Their values are defined at each switching point (each displacement extrema), not the discrete sampling time n. Hence the detected displacement amplitude u_M (which is used as a sensor signal to control the switch action) (Ji et al., 2009b), instead of the displacement u itself, is used as the error e to the FIR filter. The output y of the FIR filter is the voltage or the voltage coefficient β at the switching times, instead of the voltage value at each discrete time, and the calculated voltage is held constant until the next switching time so that a rectangular wave is generated automatically by the switching circuit. Hence the LMS-based system is a sub-system which is not executed at each discrete time, but triggered and executed at each detected extrema. The diagram of a LMS-based adaptive SSDV control system is shown in Fig. 10. In the case of the optimization of β, the value of β is calculated from

$$\beta(n') = \mathbf{h}(n') * \mathbf{u}_m(n'-1) = h(1)u_m(n'-1) + h(2)u_m(n'-2) + \cdots + h(m)u_m(n'-m) \tag{52}$$

where **h** is an FIR filter, n' is the discrete time defined at the detected extrema. This means that $n'-1$ represent the discrete time at the previous detected extremum. After β is calculate from Eq. (52), the voltage V_{cc} is obtained from Eq. (46). This method can be considered as an extension of the enhanced SSDV. In the case of the direct optimization of the voltage V_{cc}, the following equation is used:

$$V_{cc}(n') = \mathbf{h}(n') * \mathbf{u}_m(n'-1) = h(1)u_m(n'-1) + h(2)u_m(n'-2) + \cdots + h(m)u_m(n'-m)\,. \tag{53}$$

Since the voltage is directly optimized by this method, it can be considered as an improvement to the classical SSDV, where the voltage source is fixed. The same symbol **h** is used in Eqs. (52) and (53), but they have different values.
It should be noted that although the standard LMS algorithm has been used in this study, its implementation is not standard. The LMS-based is masked and executed only at the discrete time defined at the detected extrema, n', at which the FIR filter is updated and the control input is calculated. Due to the non-standard implementation, the other LMS-based control laws, such as the Filtered-X algorithm, is difficult to apply in this system.

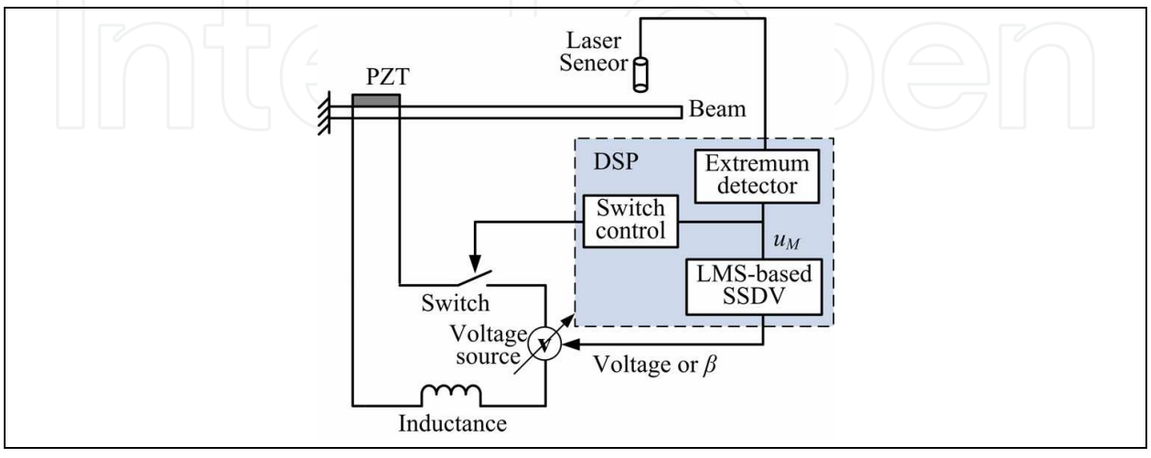

Fig. 10. The diagram of a LMS-based adaptive SSDV control system

5.3 An example of pulse-switched control

The structure used in the experiment is a cantilever GFRP (Glass Fiber Reinforced Plastics) composite beam with an embedded piezoelectric patch, as shown in Figure 11. The composite beam was made from four layers of GFRP prepreg. The GFRP prepreg and the piezoelectric patch are laminated in the following order: 0˚/90˚/90˚/PZT/0˚, where 0˚ is the length direction of the beam. The beam is 150 mm long, 51 mm wide and 0.8 mm thick and its properties are given in Table 2. The piezoelectric patch is a 30 mm × 30 mm square and its thickness is 0.2 mm. It is polarized in the thickness direction and its properties are given in Table 3. The equation of motion of the beam is a partial differential equation. The equation of motion for each mode can be obtained from a modal analysis (Ji, et al. 2008). In this study, control of the resonant vibration at the first natural frequency is considered. Hence, the amplitude of the first mode is dominant and the high-order modes can be neglected. That is, at the first resonant frequency, the structure can be simplified to a single-degree-of-freedom system, represented in Figure 1.

	GFRP
Elastic modulus E_1	$1.65\times10^{+10}$ [N/m^2]
Elastic modulus E_2	$3.52\times10^{+10}$ [N/m^2]
Poisson ratio	0.109
Shear modulus	$1.25\times10^{+10}$ [N/m^2]
Density	1800 [kg/m^3]
Thickness	0.8×10^{-3} [m]

Table 2. Material properties of the composite beam

	PZT
Elastic modulus	$59\times10^{+9}$ [N/m^2]
Poisson ratio	0.345
Density	7400 [kg/m^3]
Thickness	2×10^{-4} [m]
Piezoelectric constant d_{31}	-260×10^{-12} [m/V]
Capacitance C_p	141×10^{-9} [F]

Table 3. Material properties of the piezoelectric patch

The experimental setup is shown in Fig. 11. One end of the beam is clamped and the other is free. The piezoelectric patch is located at the clamped end, where the maximum strain is induced. The clamped end is mounted on a mini-shaker, which is used to drive the vibration of the beam. The displacement at the free end of the beam is measured by a laser displacement sensor.

The control approach is implemented in a DSP environment based on the dSPACE board DS1103. The displacement signal from the laser sensor is converted to digital and sent to the DSP system. Theoretically, the maximum displacement occurrence in the time response can be detected by comparing three consecutive points. When the noise in the displacement

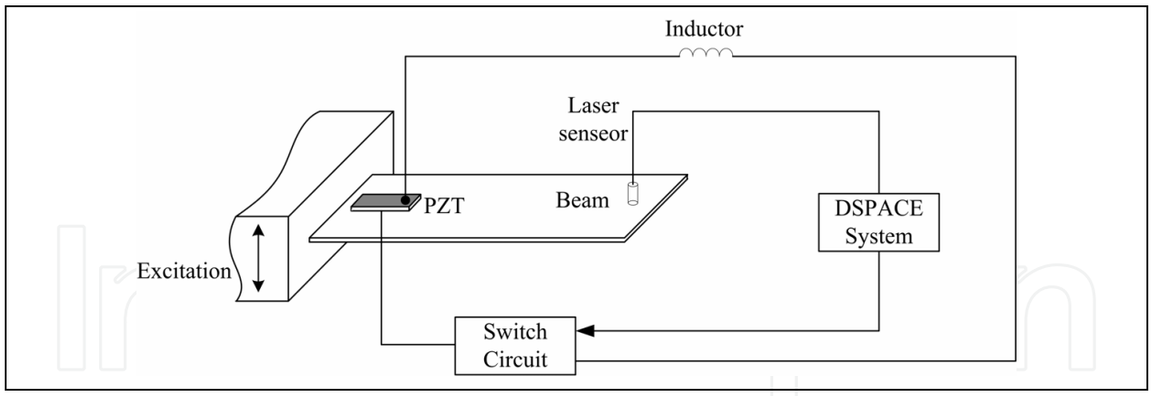

Fig. 11. Experimental setup

signal is small, this method is effective. However when the noise is relatively large, some of the obtained extrema are generated by the noise. That is, many maximum points may be obtained in a single cycle of vibration. This can lead to over-frequent switching of the circuit and induce a worsening of the control performance.

In order to prevent the system from over-frequent switching, an improved switch control algorithm has been proposed by Ji, et al. (2008). The improved algorithm turns switch to inactive state for a given period τ after each action so that no switching action can occur in this period even if extrema are detected. It can prevent the switch from over-frequent on-and-off and consequently increase the stability and performance of the control system. In this study, the improved switch control algorithm is used instead of the three-point algorithm.

The SSDI, classical SSDV, derivative-based adaptive SSDV and LMS-based adaptive SSDV methods have been used in control. Figure 12 shows the displacement curve and the voltage on the piezoelectric transducer when the voltage is not switched. The amplitude of the displacement without control is 1.6 mm and the amplitude of the voltage is 1.45 volts. Theoretically the voltage should be in phase with the displacement, but a phase difference can be observed from the figure. The phase difference may be due to the impedance of the measurement circuit connected to the piezoelectric transducer.

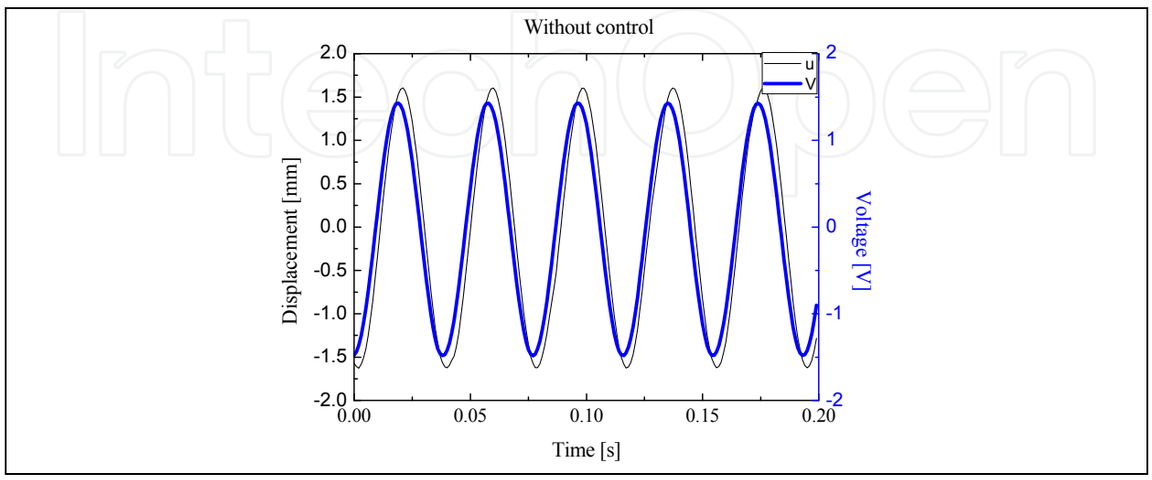

Fig. 12. Displacement of the beam and the voltage on the piezoelectric transducer

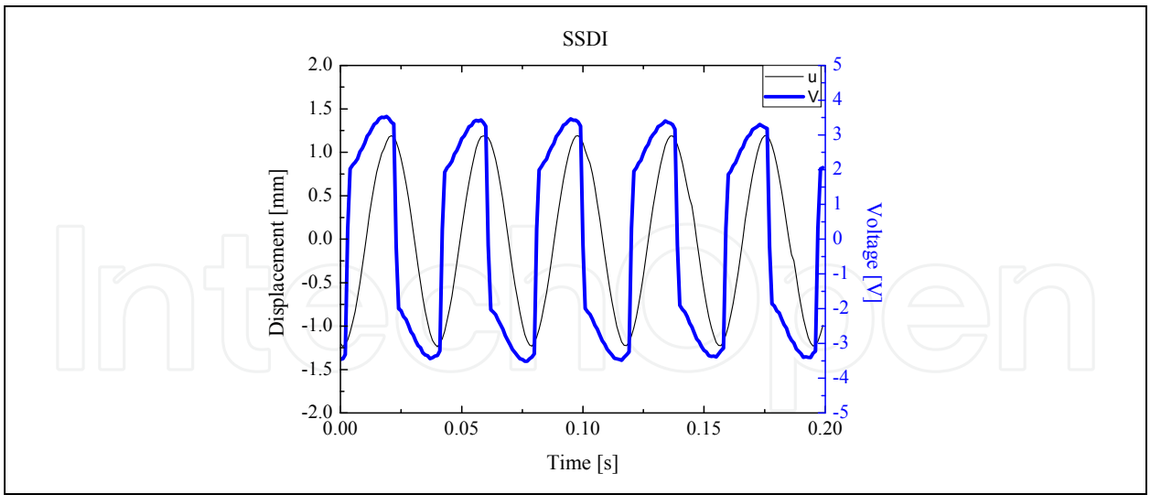

Fig. 13. Displacement of the beam and the voltage on the piezoelectric transducer with SSDI control

The result of the SSDI control is shown in Fig. 13 (Ji et al., 2008). The amplitude of voltage on the piezoelectric transducer was amplified to 3.47 volts and the displacement amplitude of vibration was reduced to 1.2 mm. It can be found that the voltage is not inverted at its extrema due to the phase difference the voltage and the displacement. The voltages before and after switching is about 3.3 volts and 1.95 volts. It means that the voltage inversion coefficient is about 0.59. For this value of inversion coefficient, the average voltage should be amplified by a factor of 2.91 when the decrease of displacement amplitude is taken into consideration. However, the average voltage was about 2.7 volts, increased only by a factor of 2.48, which corresponds to a voltage inversion coefficient of 0.43. This can be attributed to the delay of voltage inversion from its exterma.

Figure 14 shows the result of SSDV control when the voltage source V_{cc} is set to 1 volt. The amplitude of voltage on the piezoelectric transducer was raised to 5.8 volts and the

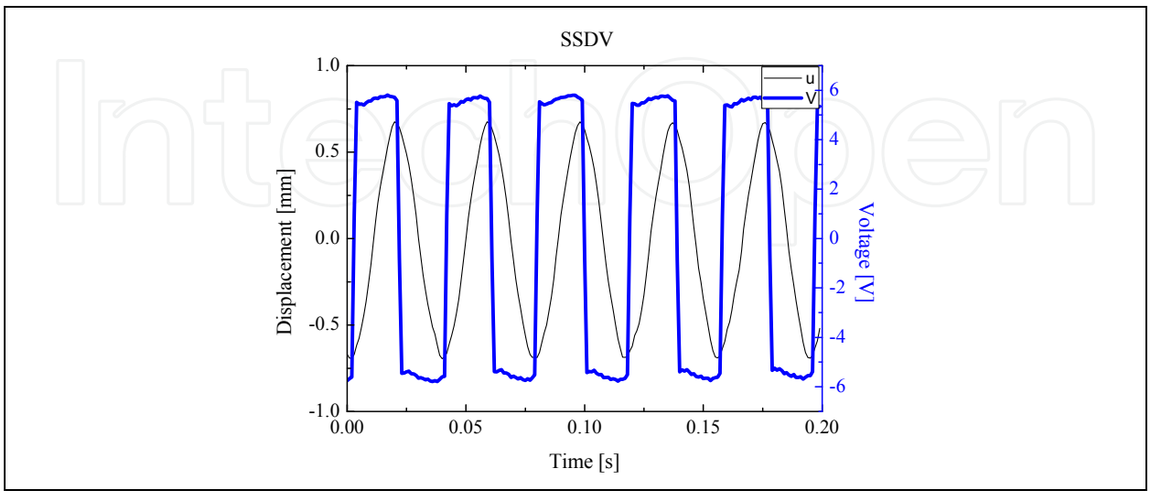

Fig. 14. Displacement of the beam and the voltage on the piezoelectric transducer with SSDV (V_{cc} = 1 Volt)

displacement amplitude was reduced to 0.67 mm. When the voltage inversion coefficient is 0.59 and the displacement reduction is taken into consideration, average voltage should be 6.2 volts, which is slightly larger than real value of 5.8 volts. When V_{cc} was set to 2.4 volts, the displacement amplitude of vibration was further reduced to 0.123 mm. However, the second resonance mode was excited slightly.

Figure 15(a) shows the displacement response of the beam when the derivative-based adaptive SSDV control was used (Ji et al., 2009b). In the derivative-based adaptive SSDV control, the voltage coefficient is optimized online and its variation with time is shown in Figure 15(b). It should be noted that the voltage coefficient β' in Fig. 15(b) and the following paragraphs is the ratio between the source voltage and the voltage of the displacement sensor and can be written as $\beta'=\alpha\beta/(C_0S_0)$, where S_0 is the sensitivity of the displacement sensor expressed by the output voltage of the sensor for unit displacement. The uncontrolled displacement amplitude is 2.0 mm. The amplitude of the first resonance mode was reduced to 0.30 mm. However, the second resonance mode was excited slightly as shown in Fig. 15(a). The results of LMS-based adaptive SSDV control, in which the voltage

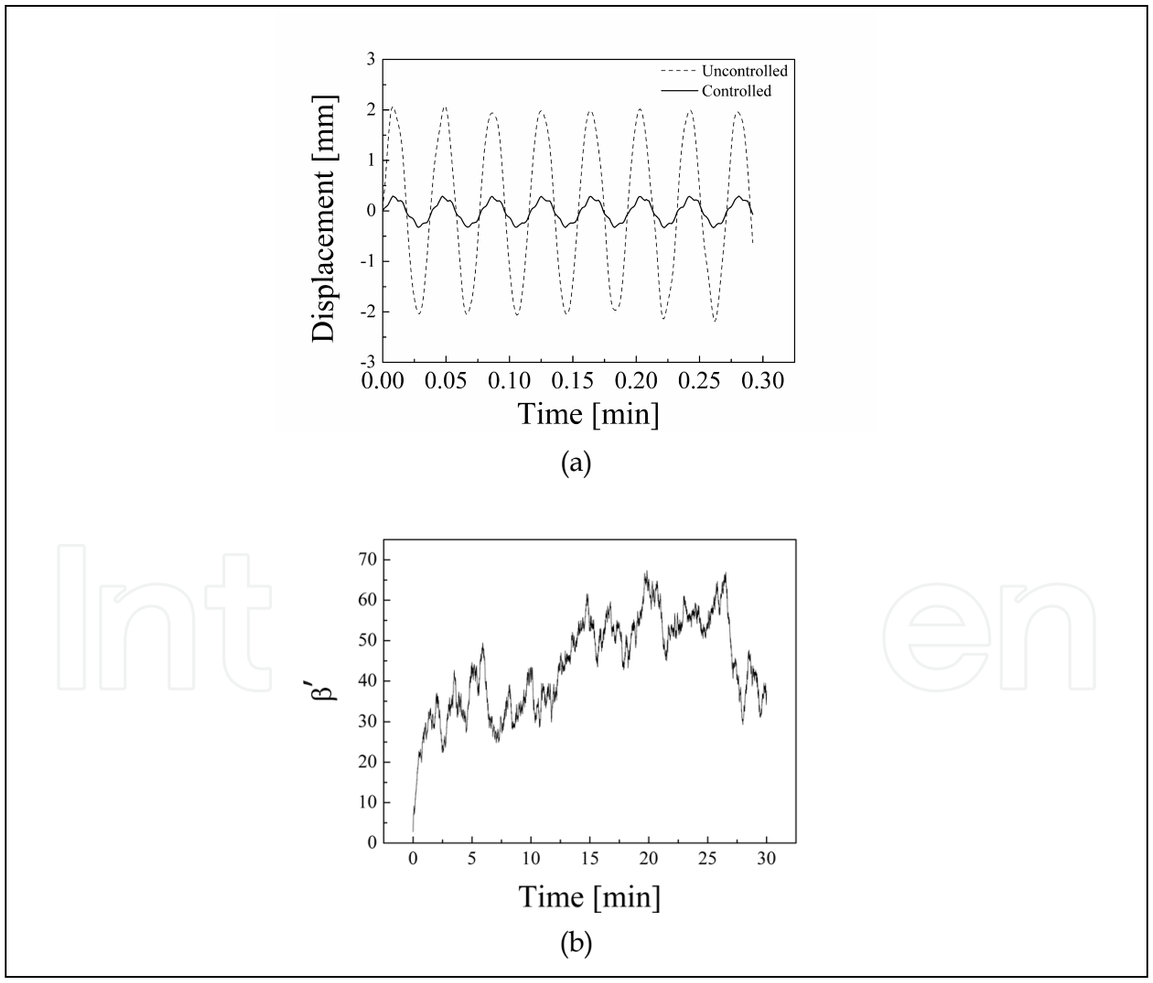

Fig. 15. Results of derivative-based adaptive SSDV (a) Displacement before and after control (b) Variation of voltage coefficient β' in thirty minutes

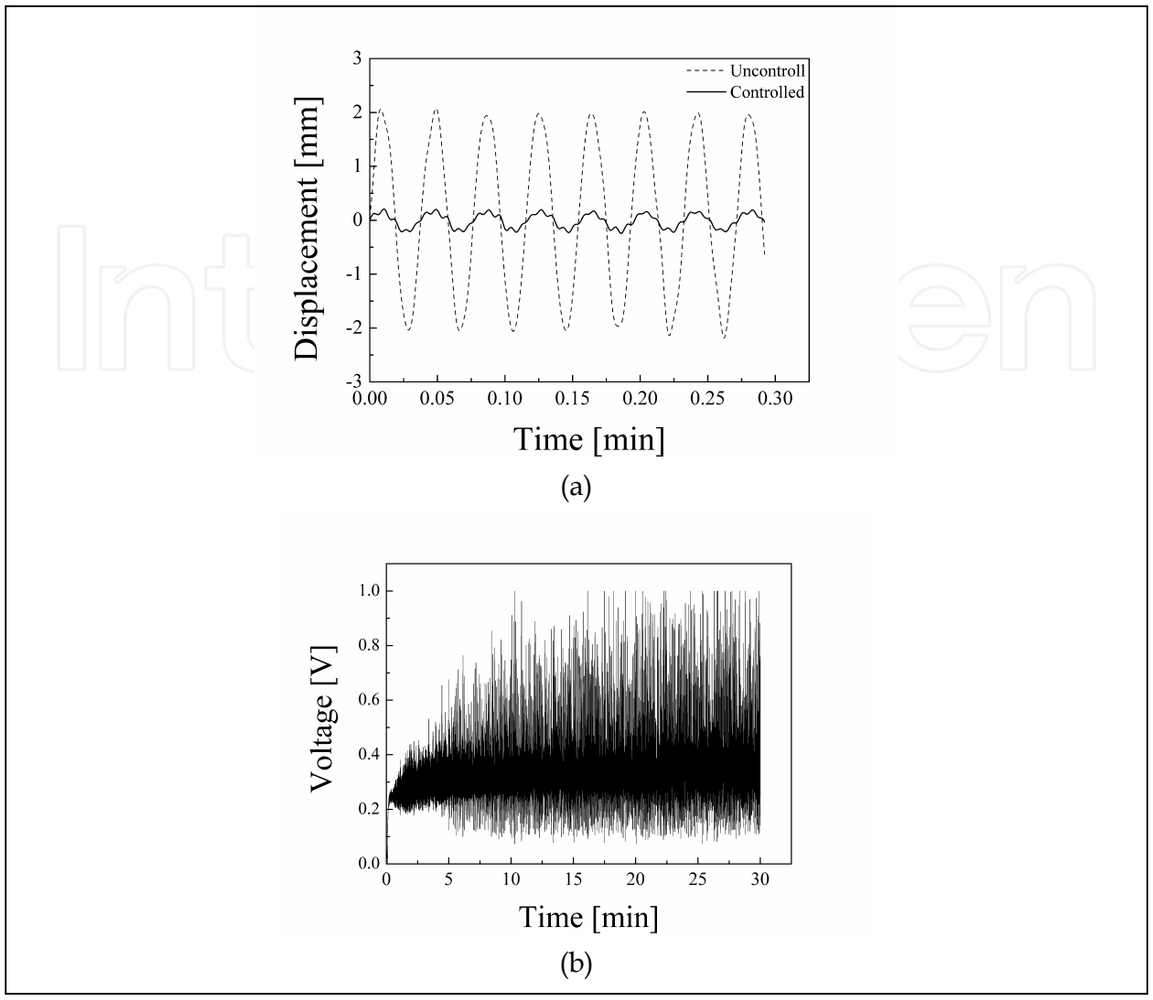

Fig. 16. Results of derivative-based adaptive SSDV (a) Displacement before and after control (b) Variation of voltage coefficient in thirty minutes

source V_{cc} was adjusted adaptively by the LMS algorithm, are show in Fig. 16. The displacement amplitude is reduced by more than 90%, from 2.0 mm to 0.19 mm. The output of the voltage source V_{cc} varies between 0.1 and 1.0 volts, with an average value of 0.355 volts. Compared with the other methods, LMS-based adaptive SSDV methods adjusting the voltage source V_{cc} output smallest voltage, but yields almost the same control performance. This means that it consumes least energy.

The control performances of different methods, including the enhanced SSDV and the LMS-based adaptive SSDV methods adjusting the voltage coefficient, are summarized in the Table 4. Although the classical SSDV method with fixed voltage source (V_{cc}=2.4V) and enhanced SSDV with (β'=150) yield the best control performance, the output of the voltage source or the value of β' must be adjusted manually by a trial and error process. Since the optimal value of the voltage source or the voltage coefficient depends on many factors, slight environmental changes may cause instability in the system with a large V_{cc} or β'. For example, when a traditional switch was used, the system became unstable when β'exceeded 50. However, the system was still stable for β'=150 when the improved switch was used.

The value of voltage is also much large than the other methods, such as the LMS-based adaptive SSDV.

Control methods	Reduction (dB)
SSDI	2.58
SSDV (V_{cc} =1V)	7.52
SSDV (V_{cc}=2.4V)	22.29
Enhanced SSDV (β'=150)	22.28
Derivative-based SSDV	16.49
LMS-based SSDV (adjusting β')	20.56
Derivative-based SSDV (adjusting V_{cc})	20.25

Table 4. Comparison of different control methods

6. Semi-active control for multi-mode damping

Though most studies in semi-active so far were devoted to single-mode control, the switching laws can be used for multi-mode control. For example, in the SSD approaches the dissipated energy reaches maximum when the voltage on a piezoelectric element is switched at each extrumum of the strain if the voltage inversion is perfect. In the method proposed by Makihara et al. (2006a, 2006b, 2007a, 2007b, 2007c), switch actions are automatically generated by the control law based on active control theories. It is applicable to multi-modal control of a structure with multiple piezoelectric transducers. However, due to the energy loss during voltage inversion, these switching laws are not optimal as demonstrated by experimental results. Better control performance can be obtained by skipping some of the switching points, which are determined from these switch control laws. Hence special switch control laws are necessary for multi-modal control.

6.1 A method considering mode selection

A multi-modal control law for a piezoceramic actuator with a switched *R-L* shunt was developed by Corr and Clark (2003) that makes use of the concepts developed for the variable mechanical spring control laws, but is less dependent on the analytical model. They based on a multimodal approach which consists in selecting the modes to be controlled and ensuring a negative rate of energy change in the selected modes of the structure. The global extracted power is derived from the global extracted energy and is given by

$$P_S = \sum_{j=1}^{N} \alpha_j \dot{\boldsymbol{u}}_j V \,. \tag{54}$$

where N is the number of modes to be controlled, u_j is modal displacement of the jth mode, and V is the voltage on the piezoelectric transducer.

If M is the set of modes to be controlled, the extracted power for the selected modes P_{SM} is given by

$$P_{SM} = \sum_{j \in M} \alpha_j \dot{\boldsymbol{u}}_j V. \tag{55}$$

The technique proposed by Corr and Clark consists in inversing the voltage at each time that the sign of $\sum_{j \in M} \alpha_j \dot{\boldsymbol{u}}_j$ change, so that P_{SM} remains always positive.

It can be noted that when the piezoelectric elements are open-circuited, the voltage V varies proportionally to $\sum_{j=1}^{N} \alpha_j u_j$, as it can be derived from

$$I = \sum_{j=1}^{N} \alpha_j \dot{\boldsymbol{u}}_j - C_0 \dot{V} \tag{56}$$

Actually $\sum_{j=1}^{N} \alpha_j u_j$ is proportional to the strain in the piezoelectric elements. If all the N modes are controlled, this method then consists in processing the piezoelectric voltage at each strain extremum, which corresponds to the earlier control law proposed for the SSD technique. They showed at the same time that the original SSD control law was not optimal in the case of wide band multimodal excitation. It can also be noted that this technique requires refined filtering devices in order to select modes to be controlled. Filtering inevitably leads to time shifts that result in a lack of effectiveness (Corr & Clark, 2003).

6.2 Methods based on probability and statistics

Guyomar and Badel (2006) proposed a new multi-mode control law for the SSD techniques based on the idea of maximizing the energy dissipated in the nonlinear processing device connected to the piezoelectric elements without taking into account any information related to the different modes of the structure. It is derived from a probabilistic description of the piezoelectric voltage. The principle of this method is that the consumption of the switching device is always zero except during the voltage inversion when it is equal to the difference of the electrostatic energy on the piezoelectric elements on the voltage inversion jump. The energy dissipated in the switching device is then given by

$$\int_0^t VIdt = \frac{1}{2} C_0 \sum_k V_k^2 (1 - \gamma^2). \tag{57}$$

where V_k is the piezoelectric voltage just before the kth inversion. It appears then that maximizing the consumption of the switching device corresponds to maximizing the sum of the squared piezoelectric voltage before each inversion. In other words, optimizing the damping corresponds to finding the switch sequence that maximizes Eq. (57).

The probabilistic approach is based on the idea of letting the voltage reach a significant but statistically probable value $\upsilon_{\min}$ before processing the voltage inversion. Since the time derivative of the extracted energy cancels when the time derivative of the strain in the piezoelectric element vanishes, the extracted energy reaches a local extremum at each extremum of the strain in the piezoelectric elements. Since strain and voltage extrema occurs at the same time, the piezoelectric voltage inversion is achieved when $V^2 > \upsilon_{\min}^2$ and V^2

reaches an extremum. $\upsilon_{\min}$ is defined after each voltage inversion so that the probability of observing $V^2 > \upsilon_{\min}^2$ is equal to P_{SW}, where P_{SW} is a fixed probability set by the user. This can be summarized in

$$P[V^2 > \upsilon_{\min}^2] = P_{SW} = 1 - F_{V^2}(\upsilon_{\min}^2). \tag{58}$$

where $\upsilon_{\min}$ can be determined using the cumulative distribution function $F_{V^2}(\upsilon_{\min}^2)$.
The critical point of this approach consists in estimating the cumulative distribution function of the voltage after each inversion. It is then easy to determine $\upsilon_{\min}$. The evolution of the piezoelectric voltage after the *k*th inversion time can be estimated using Eq. (58) where it is assumed that the strain cumulative distribution function is a slow varying function over the estimation time interval. The strain in the piezoelectric elements after the switch is thus assumed to be similar to the strain in the piezoelectric elements before the switch. The estimation is made using an observation time T_{es} of the strain. The value of T_{es} is set by the user.

$$\upsilon_{es}(t^+) = -\gamma\upsilon_k + \frac{1}{C_0}\sum_{i=1}^{N}\alpha_i(u(t^-) - u_{ik}) \quad \text{with} \begin{cases} t^+ \in [t_k, t_k + T_{es}] & \text{(future)}, \\ t^- \in [t_k - T_{es}, t_k] & \text{(past)}. \end{cases} \tag{59}$$

Experimentally, the voltage or the corresponding strain can be simply deduced from the voltage measured on an additional PZT insert left in open circuit and collocated with the principal semi-passive control PZT insert. This additional piezoelectric element is used as a strain sensor.
Recently Guyomar et al. (2007) further extended work on multi-mode vibration control based on the probability law and proposed the new control law based on a statistics. As discussed in the above, in the case of the SSD technique, the energy extracted from the structure by the piezoelectric element is proportional to $\sum \upsilon_k^2$, where υ_k is the piezoelectric voltage just before the *k*th switching sequence. This method proposed statistical analysis to define optimization instants for the switching sequence in order to maximize the extracted energy and vibration damping. It is based on a statistical evaluation of the voltage generated by the piezoelectric elements or of the structure deflection.

6.3 A method based on a displacement threshold

Although the good control performance were achieved by using the probability and statistics method, the amount of calculation of these methods are relatively larger because the probabilistic distribution of displacement or voltage in a given period needs to be calculated for switch control. Ji et al. (2009c) proposed a simpler approach for two mode control based on a displacement threshold. In this study, the following strategy is used in controlling the switch

$$\frac{du}{dt} = 0 \quad \text{and} \quad |u| > u_{cr,k}, \tag{60}$$

where $u_{cr,k}$ is the displacement threshold for switching action at time t_k. Equation (60) means that the switching actions take place at the displacement extrema which are larger than the threshold. The physical basis of this switching strategy can be explained textually as follows.

Maximum energy conversion can be realized for the high-order mode when switching action takes place at all the extrema. However the switching frequency is too high for the first mode in this case. Hence it is necessary to skip some extrema to achieve good control performance for the first mode. Generally the extrema can be divided into two categories, those with relatively large displacement amplitude and those with relatively small displacement amplitude. The extrema with relatively large amplitude are close to the extrema of the first mode. Hence switching at these extrema will yield good control performance for the first mode. On the other hand, if switching actions take place at the extrema with relatively small displacement amplitude, the control performance will deteriorate considerably due to the phase effect.

The important issue is how to decide the displacement threshold in a real system. It should be adjusted automatically according to the vibration level and control state. In this study, the amplitude threshold is calculated from average amplitude of latest ten switching points:

$$u_{cr,k} = \lambda \times \frac{1}{10} \sum_{i=1}^{10} | u(t_{k-i}) | \tag{61}$$

where t_{k-1} (i=1,…,10) is the time of the latest ten switching points and λ (0<λ<1) is a parameter that can be adjusted in the experiments. The initial value of $u_{cr,k}$ is set to zero and updated after each switching action. Because $u_{cr,k}$ is the average of the displacement at latest ten switching points, it can reasonably reflect the latest vibration level. The value of λ should be smaller than 1; otherwise the displacement at the next switching point will exceed the average displacement so that the threshold will increase infinitely.

7. Future directions

Through about ten years of research, several electronic switching circuits and switch control laws have been developed for semi-active vibration control based on switched shunt circuit. However more needs to be done in the following aspects for practical applications of these methods.

The first aspect is the switch control laws for multi-modal control. As introduced above several switch control laws have been developed for multi-mode vibration control using switched shunt circuit, but more efficient control laws are required for better control performance and higher robustness of the control system. The second aspect is the design of low-power shunt circuit. The power consumed by a switched shunt circuit is usually smaller than one milli watt, but a powerful DSP for switch control can consume much higher power. Although the power consumed by a semi-active control system is much smaller than an active control system, the energy consumption of a control system can be an important issue for some application, especially in aerospace engineering. The third aspect is development of self-powered semi-active control system. Although self-powered semi-active control systems have been developed (Niederberger & Morari, 2006; Lallart et al., 2007; Richard et al., 2007; Yabu & Onoda 2005), these systems are based on analog switch control systems, which is not so efficient for multi-mode vibration control. Hence self-powered semi-active control systems with sophisticated switch control laws are expected in the future. Since more complicated switch control laws need more powerful DSP and consumes more power,

a trade-off should also be considered between control performance and energy consumption of a semi-active control system.

8. References

Badel, A.; Sebald, G.; Guyomar, D.; Lallart, M.; Lefeuvre, E.; Richard, C. & Qiu, J. (2006). Piezoelectric vibration control by synchronized switching on adaptive voltage sources: Towards wideband semi-active damping. *Journal of Acoustics Society American*, Vol. 119, No. 5, 2815-2825.

Clark, W. W. (1999). Semi-active vibration control with piezoelectric materials as variable stiffness actuators, *Proceedings of 1000 AIAA/ASME/ASCE/AHS/ASC Structures, Structural Dynamics, and Materials Conference and Exhibit*, Vol. 3672, pp. 2623-2629.

Clark, W. W. (2000). Vibration control with state-switched piezoelectric materials. *Journal of intelligent material systems and structures*. Vol. 11, No. 4, 263-271.

Corr, L. R. & Clark, W. W. (2001). Energy dissipation analysis of piezoceramic semi-active vibration control. *Journal of intelligent material systems and structures*, Vol. 12, No. 11, 729-736.

Corr, L. R. & Clark, W. W. (2003). A novel semi-active multi-modal vibration control law for a piezoceramic actuator. *Transactions of the ASME*, Vol. 125, 214–222.

Cunefare, K. A. (2002). State-switched absorber for vibration control of point-excited beams. *Journal of Intelligent Material Systems and Structures*, Vol. 13, 97~105.

Davis, C. L.; Lesieutre, G. A. & Dosch, J. (1997). Tunable electrically shunted piezoceramic vibration absorber, *Proceedings of SPIE, Smart Structures and Materials: Passive Damping and Isolation*, pp. 51-59, San Diego, CA, 1997.

Davis, C. L. & Lesieutre, G. A. (1998). An actively tuned solid-state piezoelectric vibration absorber, *Proceedings of SPIE, Smart Structures and Materials*, Vol. 3327, pp. 169-182.

Faiz, A.; Guyomar, L.; Petit, L. & Buttay, C. (2006). Wave transmission reduction by a piezoelectric semi-passive technique. *Sensors and actuators*, Vol. 128, 230-237.

Guyomar, D.; Richard, C. & Petit, L. (2001). Non-linear system for vibration damping. *142th Meeting of Acoustical Society of America*, Fort Lauderdale, USA. 2001.

Guyomar, D. & Badel, A. (2006). Non-linear semi-passive multi-modal vibration damping: An efficient probabilistic approach. *Journal of Sound and Vibration*, Vol. 294, 249-68.

Guyomar, D.; Richard, C. & Mohammadi, S. (2007). Semi-passive random vibration control based on statistics. *Journal of Sound and Vibration*, Vol. 30, No. 7, 818-833.

Hagood, N. W.; Chung, W. H. & Flowtow, A.von. (1990). Modeling of piezoelectric actuator dynamics for active structural control. *Journal of Intelligent Material Systems and Structures*, Vol. 1, 327-353.

Hagood, N. W. & Crawley, E. F. (1991). Experimental investigations of passive enhancement of damping space structures. *Journal of Guidance, Control and Dynamics*, Vol. 14, No. 6, 1100-1109.

Hollkamp, J. J. (1994). Multimodal passive vibration suppression with piezoelectric materials and resonant shunts. *Journal of Intelligent Material Systems and Structures*, Vol. 5, 49-56.

Hopkins, M. A.; Henderson, D. A.; Moses, R. W.; Ryall, T.; Zimcik, D. G. & Spangler, R. L. (1998). Active vibration-suppression systems applied to twin-tail buffering, *Proc. SPIE Smart Structures and Materials: Industrial and Commercial Application of Smart Structures Technologies*, Vol. 3326, pp. 27-33.

Ji, H. L.; Qiu, J. H.; Zhao, Y. C. & Zhu, K. J. (2008). A study on semi-active vibration control using piezoelectric elements (in Chinese). *Journal of Vibration Engineering*, Vol. 21, No. 6, 614-619.

Ji, H. L.; Qiu, J. H.; Badel, A. & Zhu, K. J. (2009a). Semi-active vibration control of a composite beam using an adaptive SSDV approach. *Journal of Intelligent Material Systems and Structures*, Vol. 20, No. 3, 401-412.

Ji, H. L.; Qiu, J. H.; Badel, A.; Chen, Y. S. & Zhu, K. J. (2009b). Semi-active vibration control of a composite beam by adaptive synchronized switching on voltage sources based on LMS algorithm. *Journal of Intelligent Material Systems and Structures*, Vol. 20, No. 3, 939-947.

Ji, H. L.; Qiu, J. H.; Zhu, K. J.; Chen, Y. S. & Badel, A. (2009c). Multimodal vibration control using a synchronized switch based on a displacement switching threshold. *Smart Materials and Structures*, Vol. 18, No. 3, 035016: 1-8.

Ji, H. L.; Qiu, J. H.; Zhu, K. J. & Badel, A. (2010). Two-mode vibration control using nonlinear synchronized switching damping based on the maximization of converted energy. *Journal of Sound and Vibration*, Vol. 329, 2751-2767.

Kim, S.; Han, C. & Yun, C. (1999). Improvement of Aeroelastic stability of hingeless helicopter rotor blade by passive piezoelectric damping, *Proc. SPIE Smart Structures and Materials: Passive Damping and Isolation*, Vol. 3672, pp. 131-141.

Lallart, M.; Lefeuvre, E.; Richard, C. & Guyomar, D. (2007). Self-powered circuit for broadband, multimodal piezoelectric vibration control. *Sensors and Actuators A*, Vol. 143, 377-382.

Lefeuvre, E.; Guyomar, D.; Petit, L.; Richard, C. & Badel, A. (2006). Semi-passive structural damping by synchronized switching on voltage sources. *Journal of Intelligent Material Systems and Structures*, Vol. 17, No. 8/9, 653-660 (See also the Proceedings of the First Symposium on Smart Materials for Engineering and Biomedical Applications, Suzhou, China, May 16-19, 2004, published by China Aviation Industry Press.).

Makihara, K.; Onoda, J. & Minesugi, K. (2005). Low-Energy-Consumption hybrid vibration suppression based on an energy-recycling approach. *AIAA Journal*, Vol. 43, No. 8, 1706-1715.

Makihara, K.; Onoda, J. & Minesugi, K. (2006a). Novel approach to self-sensing actuation for semi-active vibration suppression. *AIAA Journal*, Vol. 44, No. 7, 1445-1453.

Makihara, K.; Onoda, J. & Minesugi, K. (2006b). Behavior of piezoelectric transducer on energy-recycling semi-active vibration suppression. *AIAA Journal*, Vol. 44, No. 2, 411-413.

Makihara, K.; Onoda, J. & Minesugi, K. (2007a). A self-sensing method for switching vibration suppression with a piezoelectric actuator. *Smart Materials and Structures*, Vol. 16, No. 2, 455-461.

Makihara, K.; Onoda, J. & Minesugi, K. (2007b). Using tuned electrical resonance to enhance bang-bang vibration control. *AIAA Journal*, Vol. 45, No. 2, 497-504.

Makihara, K.; Onoda, J. & Minesugi, K. (2007c). Comprehensive assessment of semi-active vibration suppression including energy analysis. *Journal of Vibration and Acoustics, Transactions of the ASME*, Vol. 129, 84-93.

Niederberger, D. & Morari, M. (2006). An autonomous shunt circuit for vibration damping. *Smart Material and Structure*, Vol. 15, 359-364.

Onoda, J., Oh, H.-U., & Minesugi, K. (1997), Semiactive Vibration Suppression with Electrorheological-Fluid Dampers, *AIAA Journal*, Vol. 35, No. 12, 1844–1852.

Onoda, J.; Makihara, K. & Minesugi, K. (2003). Energy-recycling semi-active method for vibration suppression with piezoelectric transducers. *AIAA Journal*, Vol. 41, No. 4, 711-719.

Petit, L.; Lefeuvre, E.; Richard, C. & Guyomar, D. (2004). A broadband semi passive piezoelectric technique for structural damping, *Proceedings of SPIE International Symposium on Smart Structures and Materials: Damping and Isolation*, San Diego, CA, USA. 2004.

Qiu, J.; Ji, H. & Zhu, K. (2009). Semi-active Vibration Control Using Piezoelectric Actuators in Smart Structures, *Frontier of Mechanical Engineering in China*, Vol. 4, No. 3, 242-251.

Richard, C.; Guyomar, D.; Audigier, D. & Ching, G. (1999). Semi-passive damping using continuous switching of a piezoelectric device, *Proceedings of the SPIE Smart Structures and Materials Conference: Passive Damping and Isolation*, San Diego, 1999, Vol. 3672, 104-111.

Richard, C.; Guyomar, D.; Audigier, D. & Bassaler, H. (2000). Enhanced semi passive damping using continuous switching of a piezoelectric device on an inductor, *Proceedings of SPIE International Symposium on Smart Structures and Materials: Damping and Isolation*, Vol. 3989, 288-299.

Richard, C.; Guyomar, D. & Lefeuvre, E. (2007). Self-powered Electronic Breaker with Automatic Switching by Detecting Maxima or Minima of Potential Difference Between its Power Electrodes Patent # PCT/FR2005/003000, publication number: WO/2007/063194, 2007.

Simpson, J. & Schweiger, J. (1998). Industrial Approach to Piezoelectric Damping of Large Fighter Aircraft Components, *Proc. SPIE Smart Structures and Materials: Industrial and Commercial Application of Smart Structures Technologies*, Vol. 3326, pp. 34-46.

Shen, H.; Ji, H. L.; Qiu, J. H. & Zhu, K. J. (2009). A Semi-passive Vibration Damping System Powered by Harvested Energy. *International Journal of Applied Electromagnetics and Mechanics*, Vol. 31, No. 4, 219-233.

Wu, S.; Turner, T. L. & Rizzi, S. A. (2000). Pizoelectric Shunt Vibration Damping of an F-15 Panel under High-acoustic Excitation, *Proc. SPIE Smart Structures and Materials: Damping and Isolation*, Vol. 3989, pp. 276-287.

Wang, K. W.; Lai, J. S. & Yu, W. K. (1996). Energy-based parametric control approach for structural vibration suppression via semi-active piezoelectric networks. *Transaction of ASME, Journal Vibration and Acoustics*, Vol. 115, 505-509.

Yabu, T. & Onoda, J. (2005). Non-power-supply semi-active vibration suppression with piezoelectric actuator (in Japanese), *Proceedings of the JSASS/JSME Structures Conference*, Vol. 47, pp. 48-50.

Zhang, J. M.; Chang, W.; Varadan, V. K. & Varadan, V. V. (2001). Passive underwater acoustic damping using shunted piezoelectric coatings. *IOP Journal of Smart Materials and Structures*, Vol. 10, 414-420.

Vibration Control

Edited by MickaÃƒÂ«l Lallart

ISBN 978-953-307-117-6
Hard cover, 380 pages
Publisher Sciyo
Published online 18, August, 2010
Published in print edition August, 2010

Vibrations are a part of our environment and daily life. Many of them are useful and are needed for many purposes, one of the best example being the hearing system. Nevertheless, vibrations are often undesirable and have to be suppressed or reduced, as they may be harmful to structures by generating damages or compromise the comfort of users through noise generation of mechanical wave transmission to the body. the purpose of this book is to present basic and advanced methods for efficiently controlling the vibrations and limiting their effects. Open-access publishing is an extraordinary opportunity for a wide dissemination of high quality research. This book is not an exception to this, and I am proud to introduce the works performed by experts from all over the world.

InTech Europe
University Campus STeP Ri
Slavka Krautzeka 83/A
51000 Rijeka, Croatia
Phone: +385 (51) 770 447
Fax: +385 (51) 686 166
www.intechopen.com

InTech China
Unit 405, Office Block, Hotel Equatorial Shanghai
No.65, Yan An Road (West), Shanghai, 200040, China
中国上海市延安西路65号上海国际贵都大饭店办公楼405单元
Phone: +86-21-62489820
Fax: +86-21-62489821

IntechOpen